ChemistryOPEN

Supporting Information

Hierarchical SAPO-34 Architectures with Tailored Acid Sites using Sustainable Sugar Templates

Ivana Miletto,[a] Chiara Ivaldi,[a] Geo Paul,[a] Stephanie Chapman,[b] Leonardo Marchese,[a] Robert Raja,[b] and Enrica Gianotti*[a]

open_201800001_sm_miscellaneous_information.pdf

Supporting Information

Experimental

Microporous SAPO-34 synthesis

Aluminium isopropoxide (7.00g, Sigma Aldrich) was added slowly to tetraethylammonium hydroxide (TEAOH) (14.00 ml, 35wt% in H_2O, Sigma Aldrich) under stirring. Deionized water (21 ml) was added and the mixture was stirred for 1 h. Tetraethylorthosilicate (TEOS) (1.14 ml, Sigma Aldrich) was added dropwise under stirring and the mixture was further stirred for 2 h. Phosphoric acid (2.33 ml, 85wt% in H_2O, Sigma Aldrich) was added dropwise under stirring. The gel was vigorously stirred for 30 min to produce a white gel with the following composition:

1.0 Al: 1.0 P: 0.15 Si: 1 TEAOH: 50 H_2O

The gel was transferred to a Teflon-lined stainless-steel autoclave and crystallized at 473K for 60 h under autogenous pressure. The solid product from autoclave was then recovered by filtration and washed with water. The as-prepared product was dried in air at 373K and calcined in a tube furnace under air flow at 873K for 16h to produce a white crystalline solid.

Characterization methodologies

Before undertaking structural, volumetric and spectroscopic analysis, calcined samples were outgassed at 573K to remove adsorbed water.

Scanning Electron Microscopy (SEM) images at different magnifications were recorded on a Quanta 200 FEI Philips Scanning Electron Microscope equipped with an EDAX energy dispersive spectroscopy (EDS) attachment. The electron source was a tungsten filament operating at 25 keV. The samples were coated with a thin gold layer to ensure surface conductivity.

X-ray powder diffraction (XRD) patterns were obtained using an ARL XTRA48 diffractometer with Cu Kα radiation (λ = 1.54062 Å).

For ICP-OES analyses, samples were digested under acidic conditions before being aspirated into the Varian Vista MPX CCD Simultaneous axial ICP-OES instrument.

N_2 physisorption measurements were carried out at 77 K in the relative pressure range from $1x10^{-6}$ to 1 P/P_0 by using a Quantachrome Autosorb1MP/TCD instrument. Prior to the analysis, the samples were outgassed at 573 K for 3 h (residual pressure lower than 10^{-6} Torr). Specific surface areas were determined using the BET equation, in the relative pressure range from 0.01 to 0.1 P/P_0. The desorption branch of the N_2 physisorption isotherm was analyzed by means of the NLDFT (non-local density functional theory) method, to obtain the pore size distribution of the materials.

Thermogravimetric analyses (TGA/DTG) of materials were performed under argon flow (100 mL min ^{1}) with a SETSYS Evolution TGA-DTA/DSC thermobalance, heating from 40 to 1000 1C at 5 1C min ^{1}.

Solid-state (SS) NMR spectra were acquired on a Bruker Avance III 500 spectrometer and a wide bore 11.7 Tesla magnet with operational frequencies for ^{1}H, ^{29}Si, ^{31}P and ^{27}Al of 500.13, 99.35, 202.45 and 130.33MHz, respectively. A 4mm triple resonance probe with magic angle spinning (MAS) was employed in all the experiments and the samples were packed on a Zirconia rotor and spun at a MAS rate of 15 kHz. The magnitude of radio frequency fields, μ_{rf}, were 100, 83 and 42 kHz for ^{1}H, ^{31}P and ^{29}Si, respectively. The ^{27}Al MAS spectra were acquired on large sweep width with small pulse angle (π/12) to ensure quantitative interpretation. In the case of ^{29}Si, ^{31}P and ^{27}Al MAS NMR, high-power proton decoupling was applied. The relaxation delay, d1, between accumulations was 5, 1, 20, and 60 s for ^{1}H, ^{27}Al, ^{31}P and ^{29}Si MAS NMR spectroscopy, respectively. All chemical shifts were reported by using δ scale and are externally referenced to TMS for ^{1}H and ^{29}Si NMR, $Al(H_2O)_6^{3+}$ ion in 1.0 m $AlCl_3$ solution for ^{27}Al NMR and H_3PO_4 (85%) for ^{31}P NMR. The chemical shifts reported for ^{27}A1 are not corrected for second-order quadrupole effects.

^{1}H MAS NMR spectra were fitted with DMFIT functions for quantitative deconvolution of overlapping peaks. The samples were packed on a NMR rotor and dehydrated at 573K under vacuum ($1x\ 10^{-4}$ mbar) for 2 h prior to the loading into the magnet and recording of the NMR spectrum.

FTIR spectra of self-supporting pellets were collected under vacuum conditions (residual pressure $<10^{-5}$ mbar) using a Bruker Equinox 55 spectrometer equipped with a pyroelectric detector (DTGS type) with a resolution of 4 cm^{-1}. NH_3, 2,4,6-trimethylpyridine (2,4,6-TMP,

collidine) were adsorbed at room temperature using specially designed cells permanently connected to a vacuum line to perform adsorption–desorption *in situ* measurements. FTIR spectra were normalized with respect the pellet weight and, whenever specified, are reported in difference-mode by subtracting the spectrum of the sample in vacuum from the spectrum of the adsorbed molecules.

The total number of accessible Brønsted acid sites (N) was estimated using the Lambert–Beer law in the form $A = \varepsilon N \rho$, where A is the integrated area of the bands of the protonated species, ε is the molar extinction coefficient ($cm^2\ mmol^{-1}$), N is the concentration of the vibrating species ($mmol\ g^{-1}$), and ρ is the density of the disk (mass/area ratio of the pellet, $mg\ cm^{-2}$). The accessibility factor (AF) is defined as the number of Brønsted sites detected by 2,4,6-TMP adsorption, divided by the total number of Brønsted acid sites detected by ammonia adsorption

Catalysis

A portion of calcined catalyst was degassed by heating overnight at 120°C under vac- uum. A 3-neck glass-lined reactor was charged with cyclohexanone oxime (0.1 g, Sigma Aldrich), anhydrous chlorobenzene (internal standard, 0.1 g, Sigma Aldrich), dried catalyst (0.1 g), and anhydrous benzonitrile (20 ml, Sigma Aldrich). The reaction vessel was sealed with a rubber septum, glass stopper, and reflux condenser. The reaction was transferred to a pre-heated oil bath at 130 °C and stirred at this temperature, under constant nitrogen atmosphere. Aliquots of the reaction mixture were extracted hourly over a 6 hour reaction period and analysed by gas chromatography using the Clarus 480 apparatus with flame ionisation detector (FID) and an Elite 5 column. Products were identified using authenticated standards and quantified against the internal standard, chlorobenzene.

Table S1. Textural properties of the hierarchical and microporous SAPO-34.

	GLU-S01	FRU-S02	SUC-S03	microSAPO-34
S_{BET} /m^2 g^{-1}	316	554	554	477
S_{DFT} /m^2 g^{-1}	691	968	808	819
S_{micro} /m^2 g^{-1}	662	853	590	811
[a]S_{meso} /m^2 g^{-1}	29	115	118	8
[b]Relative mesopore area [%]	4.20	11.90	14.60	0.98
$V_{tot\ DFT}$ /cm^3 g^{-1}	0.24	0.41	0.36	0.26
V_{micro} /cm^3 g^{-1}	0.20	0.22	0.17	0.23
V_{meso} /cm^3 g^{-1}	0.04	0.20	0.19	0.03
[c]Relative mesopore volume [%]	16.7	48.8	52.8	11.5

[a]$S_{meso} = S_{DFT} - S_{micro}$; [b]Relative mesopore area = S_{meso}/S_{DFT} x 100 ; [c]Relative mesopore volume= $V_{meso}/V_{tot\ DFT}$ x 100

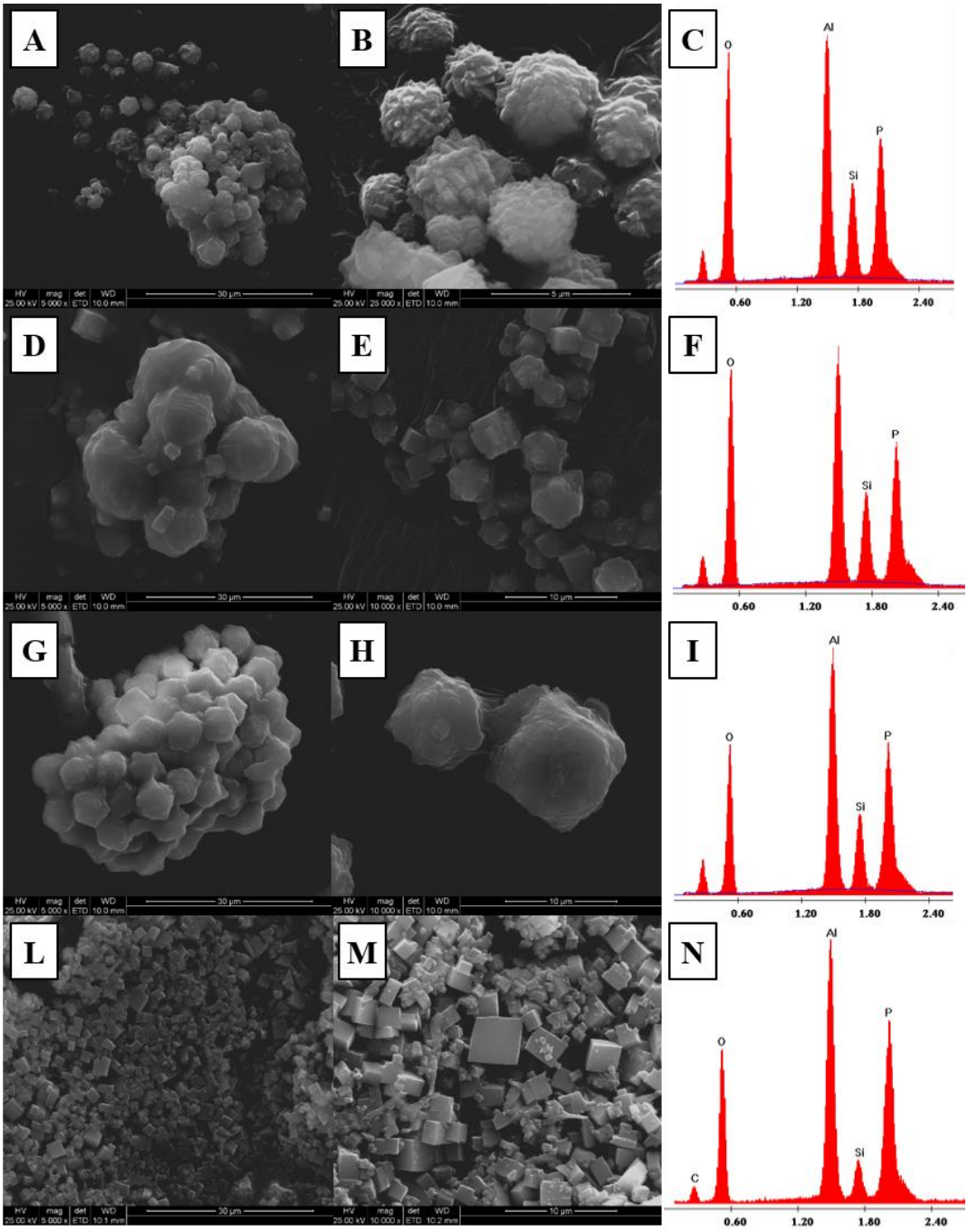

Figure S1. Representative SEM image of GLU-S01 (A, B), FRU-S02 (D, E), SUC-S03 (G, H), microporous SAPO-34 (L, M) and energy-dispersive X-Ray spectroscopic microanalysis (EDX) of GLU-S01 (C), FRU-S02 (F), SUC-S03 (I) and microporous SAPO-34 (N).

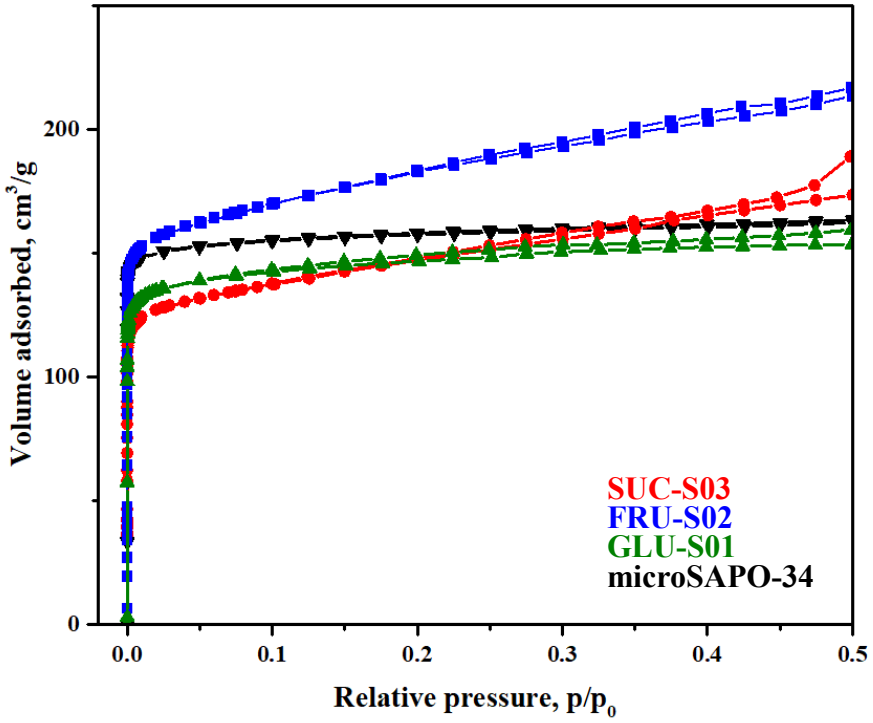

Figure S2 The N_2 adsorption/desorption isotherms at 77K in the low p/p_0 region (zoom of Fig.1B).

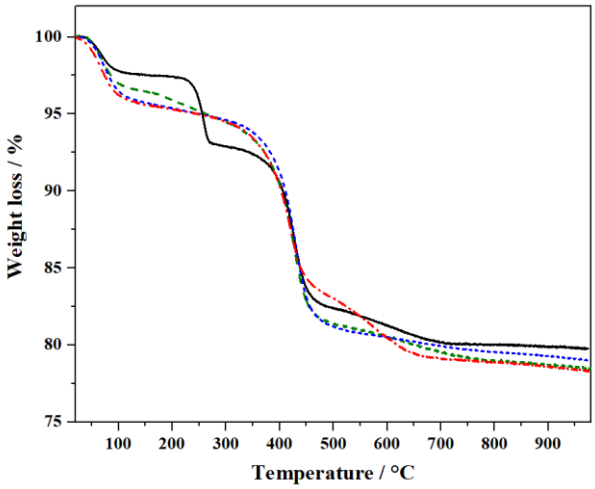

Figure S3. TGA curves of GLU-S01 (green curve/dash), FRU-S02 (blue curve/short dash), SUC-S03 (red curve/dash dot) and microporous SAPO-34 (black curve/plain).

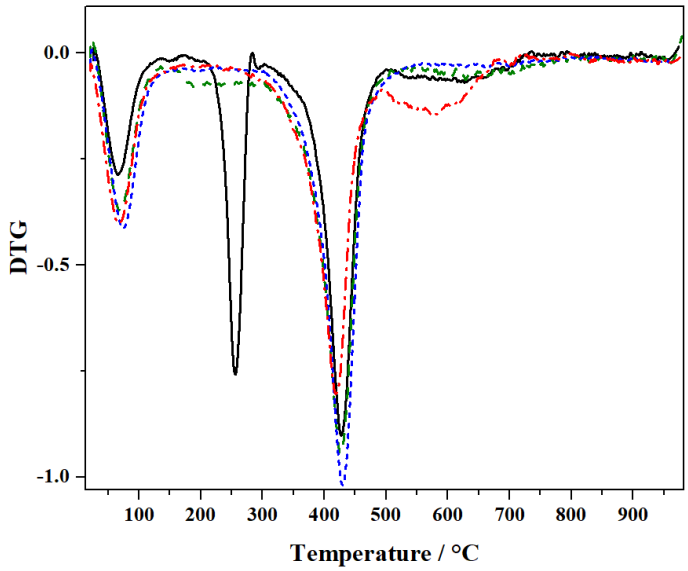

Figure S4. DTG curves of GLU-S01 (green curve/dash), FRU-S02 (blue curve/short dash), SUC-S03 (red curve/dash dot) and microporous SAPO-34 (black curve/plain).

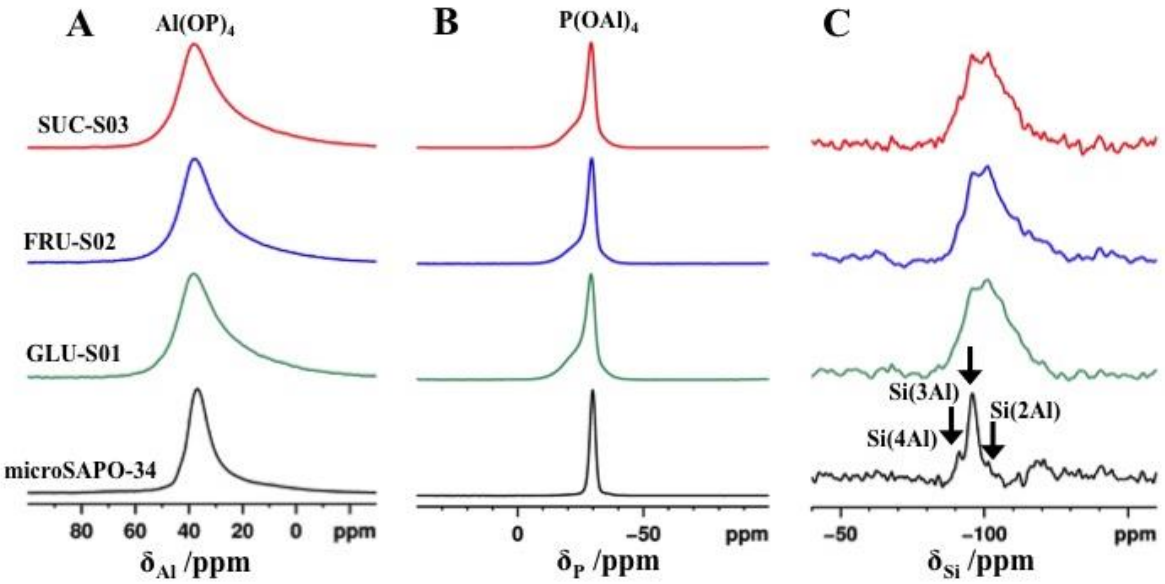

Figure S5 - The ^{27}Al (A), ^{31}P (B) and ^{29}Si (C) MAS NMR spectra of calcined hierarchical GLU-S01 (green), FRU-S02 (blue), SUC-S03 (red) and microporous SAPO-34 (black).

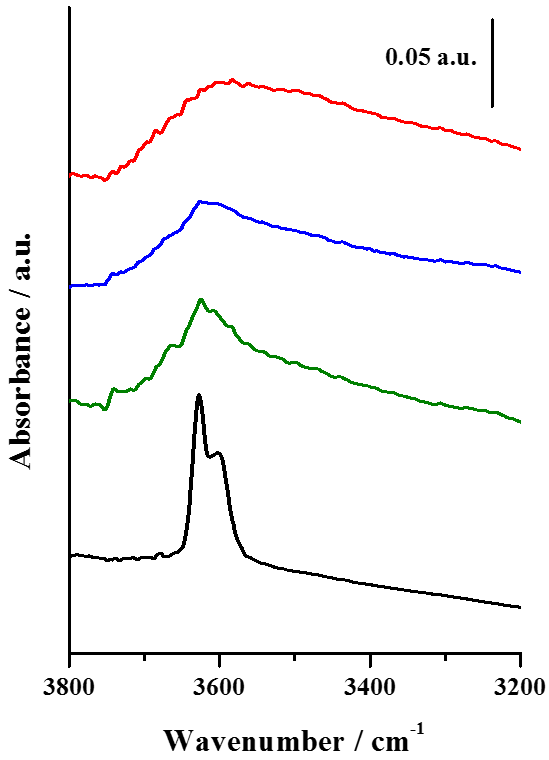

Figure S6. FTIR spectra in the OH stretching region of calcined microporous SAPO-34 (black) and hierarchical GLU-S01 (green), FRU-S02 (blue) and SUC-S03 (red). FTIR spectra of hierarchical SAPO-34 are affected by the high scattering profile in the O-H stretching region of the spectrum.